International Journal of Chemistry and Technology

http://dergipark.org.tr/ijct

Research Article

Investigation of Theoretical Properties of Axially Disubstituted Silicon (iv) Phthalocyanine Compound by Computational Chemistry

(ID) Aslıhan Aycan TANRIVERDİ[1] *   (ID) Ümit YILDIKO[2]

[1]*Department of Chemistry, Faculty of Science and Letters, Kafkas University, Kars, Türkiye*

[2]*Department of Bioengneering, Faculty of Engineering and Architecture, Kafkas University Kars, Türkiye*

*Corresponding author e-mail: t.aslihanaycan@gmail.com

Citation: Tanrıverdi A.A.; Yıldıko, Ü. *Int. J. Chem. Technol.* **2025**, 9(1), 25-35.

ABSTRACT

The electronic properties of phthalocyanine compound were investigated by computational chemistry. These quantum chemical studies are expected to contribute to the development of new solar cells. The energy and photophysical characteristics of the Si-Pc derivative were investigated through quantum chemical studies using density functional theory (DFT) and time-dependent DFT (TD-DFT) approaches. In addition, the following global descriptor types were estimated: hardness (η), electron affinity (EA), bandgap energies (Egap), ionisation potential (IP), highest occupied molecular orbital (HOMO), lowest unoccupied molecular orbital (LUMO) and electrophilicity index (Ω). The theoretical results in this regard agree well with DFT approaches.

Keywords: Axially phthalocyanine, DFT, ELF, bandgap, renewable energy.

----

1. INTRODUCTION

The field of photonics, the science and technology of using light, is constantly expanding due to the identification of new photonic properties and the development of novel technologies.[1,2] In addition to making devices more mechanically flexible for so-called flexible applications, this also reduces the value of the material budget and increases the efficiency of photovoltaic (PV) properties.[3] The combination of flexibility and cost-effectiveness of solution-processed organic photovoltaic devices makes them a valuable alternative to traditional solar cells.[4] As research and development in this area continues, it is becoming increasingly evident that OPV devices have the potential to play a significant role in the future of solar power generation. Phthalocyanines (Pcs) have garnered significant attention in the field of solar cell applications.[5,6] Their unique properties make them particularly suitable for harnessing solar energy effectively. One of the primary advantages of

phthalocyanines is their efficient absorption band in the near-infrared (NIR) region, which is crucial for maximizing the energy harvested from sunlight.[7] On the other hand, despite the advantageous properties of phthalocyanines (Pcs) in solar cell applications, they face significant challenges due to their strong π-π intermolecular interactions among the planar Pc cores.[8] These interactions result in the aggregation of Pcs, leading to a notable decrease in their solubility in common organic solvents. Consequently, while the electronic properties of phthalocyanines (Pcs) can be fine-tuned for improved performance in solar cell applications, there remains significant potential to further enhance the solubility of these compounds.[9] An effective strategy for achieving this is to introduce bulky groups at the peripheral positions of the Pc macrocycle. This approach aims to suppress macrocycle aggregation, thereby increasing the solubility of the materials overall. Many phthalocyanine (Pc) derivatives have been systematically examined to determine their potential as

electron donor or acceptor constituents in organic photovoltaic (OPV) solar cells.[10] A comprehensive study highlights the potential of PCs to improve the efficiency of solar energy conversion.[11]

The bulky axial substituents on Si-Pc derivatives play a crucial role in mitigating the strong π-π intermolecular interactions that typically lead to aggregation in phthalocyanine materials.[12] By introducing steric hindrance, these substituents disrupt the close packing of the planar macrocycles, allowing for a more homogeneous distribution of the Si-Pc derivatives within the active layer. This improved morphology is vital for enhancing charge transport and minimizing recombination losses, thereby increasing the overall efficiency of the OPV device. These studies found that the phase-separated morphology of the active layer, charge-carrier mobility, HOMO-LUMO energy levels, and light-harvesting capacity are important variables that influence the power conversion efficiency of phthalocyanine-based organic photovoltaic (OPV) solar cells.[13]

However, studies on the characterization of semi-metal complexes and the application of DFT and time-dependent density functional theory (TD-DFT) are underway.[14] In the last 20 years, DFT and TD-DFT have come to be considered the most popular electronic structure measuring systems for various applications.[15] It is very significant to understand high-efficiency energy transfer to design devices that will solve the energy transfer problem.[16] This has been implemented as a molecular example in solar cells to achieve the fundamental properties of electronic excitation.[17] In calculations based on TD-DFT, the value giving a distinct peak on the high-energy section of the Q band should support the electronic spectrum near the ultraviolet-visible light region. As is known, electronic transitions are defined in the Q band region. A guess must be made here.[18] Also, the quantitative difference between the experimental data and the B-band depends on the applied base set and functionality.[19] The Q-band must physically depend on the four orbital patterns as a result of the indivisible, derived metal or semimetal symmetry in the light absorption spectrum.[20] The Electron localization function (ELF) analysis is a well-defined function with a pragmatic nature, but it is also a powerful means for researching the temperament of the chemical bond.[20-22]

In this work, our group synthesized an axially substituting bis(3-chloropropanoate), which was carried out using phthalocyanine compound[23] significant parameters of Si-Pc were researched by computational chemistry. The energy and surface features of the molecule were calculated via DFT and TD-DFT studies. Quantum studies on this phthalocyanine compound aim to understand how its electronic properties can be

modified to make it more suitable for solar cells, thus taking an important step towards developing more efficient and cost-effective solar cells.

2. MATERIALS AND METHODS

2.1. Simulations of All Theoretical Studies

The Si-Pc input file was transferred to Gaussian 09 W (revision B.01) software to calculate the DFT and TD-DFT methods.[24] Next, basis sets for B3LYP/6-311G (d, p), B3PW91/6-31G'(d,p), and mPW1PW91/6-31G (d,p) hybrid density functionals were employed (in DFT). B3LYP (Becke's three-parameter Lee-Yang-Parr functional) is a widely used hybrid functional that combines Becke's three-parameter modified general exchange functional with the Lee-Yang-Parr correlation functional. Due to its broad applicability, B3LYP is extensively employed in various fields, particularly in structural optimization and energy calculations of organic molecules. B3PW91 (Becke's three-parameter Perdew-Wang 91 functional) is a variant of B3LYP that replaces the Lee-Yang-Parr correlation functional with the Perdew-Wang 91 functional. The PW91 functional introduces a distinct approach to exchange and correlation, making it more suitable for the computation of complex systems, such as transition metal complexes and systems requiring strong correlation effects. MPW1PW91 (Mixed Perdew-Wang 91 hybrid functional) is a hybrid adaptation of the Perdew-Wang 91 functional. Unlike B3LYP and B3PW91, MPW1PW91 aims to more accurately account for the imbalance between exchange and correlation energies, providing improved performance in certain molecular simulations. Furthermore, the TD-DFT B3LYP / 6-311G (d, p) polarized basis set was employed. The Gauss View 6.0 program was used to visualize the MEPS of the methods. Then, checkpoint file was prepared for the DFT-B3LYP/6-311G.[25] The Multiwfn 3.8 version application was used to create the ELF (http://www.whxb.pku.edu.cn/EN/10.3866/PKU.WHX B20112786) graphical image using these files.

B3LYP is one of the most widely used hybrid functionals for structural optimization and energy calculations of organic molecules. It generally provides reasonable accuracy in predicting photonic properties such as UV-Vis spectra (via TD-DFT), HOMO–LUMO energy levels, and molecular orbital analyses. B3PW91, similar to B3LYP, employs Becke's three-parameter exchange functional, but replaces the Lee–Yang–Parr correlation functional with the Perdew–Wang 91 (PW91) functional. The PW91 functional treats electron correlation differently, which can be advantageous for systems that require a more sophisticated treatment of correlation effects, such as transition metal complexes. It offers an alternative perspective, especially for more accurate prediction of excited molecular states.

mPW1PW91 was developed to better address the imbalance between exchange and correlation energies. It is known to yield more accurate results than B3LYP in TD-DFT calculations of excited states, particularly for $\pi \rightarrow \pi^*$ transitions. The 6-311G(d,p) and 6-31G'(d,p) basis sets incorporate polarization functions (d and p), which enhance sensitivity to the directional characteristics of electron density. These basis sets enable a more accurate representation of orbital interactions necessary for describing photonic properties, especially in excited state analyses. The 6-311G(d,p) basis set is larger and more detailed, making it suitable for the accurate determination of energy levels and transition energies. In contrast, 6-31G'(d,p) is a more computationally efficient alternative that still provides satisfactory accuracy, making it preferable for larger systems.

3. RESULTS AND DISCUSSION

3.1. HOMO-LUMO and Q-B bands

The photonic and electrical properties of materials are often analyzed using HOMO (Highest Occupied Molecular Orbital) and LUMO (Lowest Unoccupied Molecular Orbital) energy levels, which play a critical role in determining quantum chemical behavior.[26,27] In general, HOMO-LUMO dissociation occurs by the effect of intermolecular charge transmit to electron-accepting groups from electron-donating groups.[28] It decides to take into account the small energy gap between orbitals, in fact, it also provides high reactivity during the inter-orbital transition.[29,30] The energies of molecular orbitals were computed in the TD-DFT system for the electronic absorption spectrum (Figure 1). The energies of the molecular orbitals were successfully obtained. Table 1 presents information on the electronic energy parameters of Si-Pc.
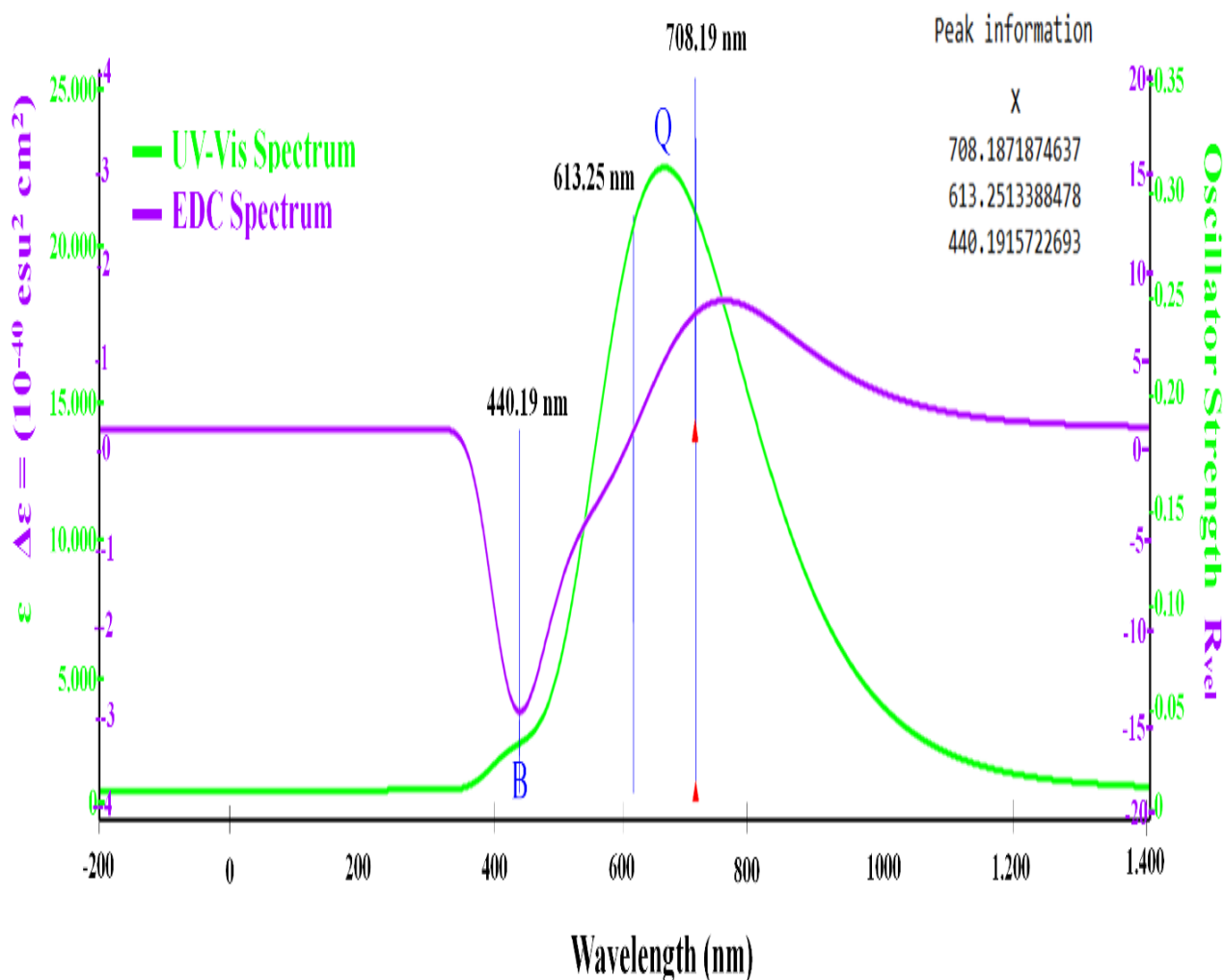

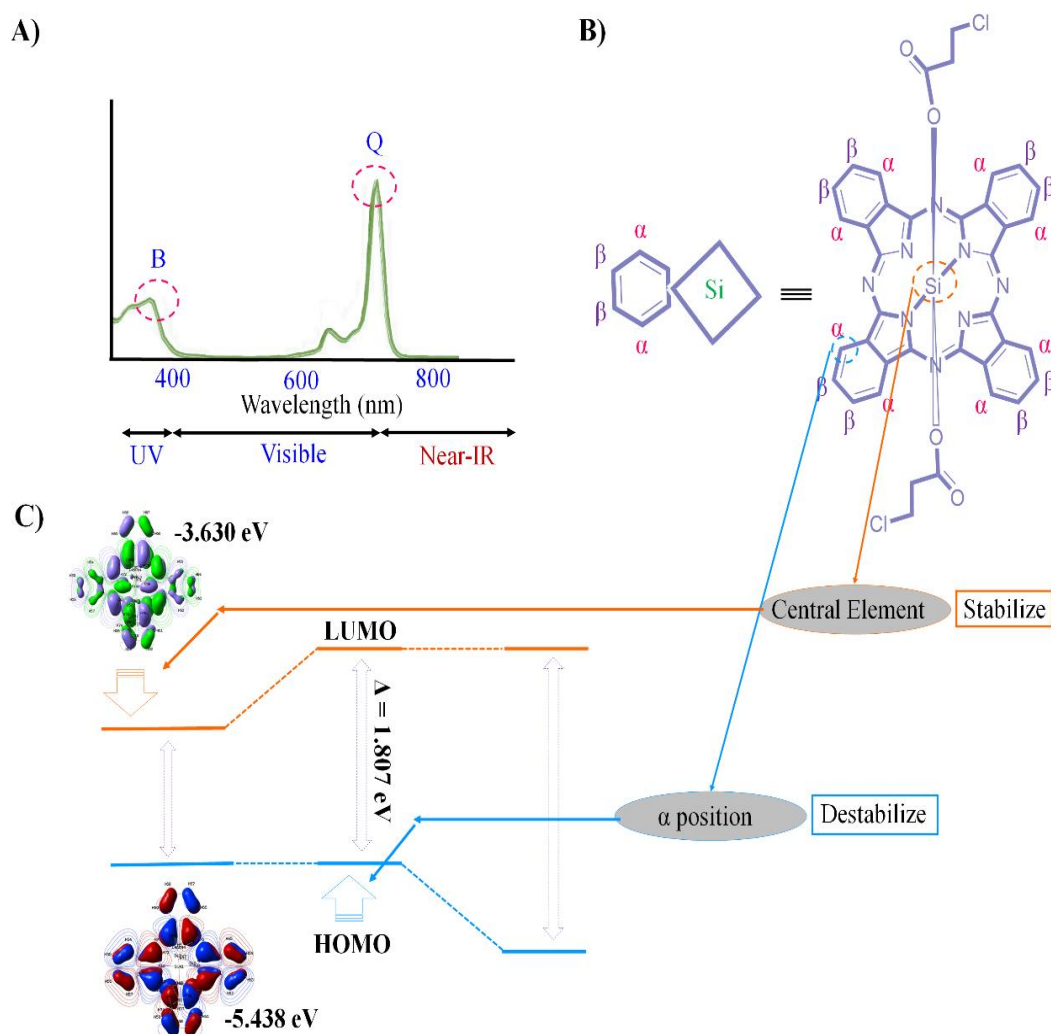**Figure 1.** Electronic absorption spectrums of Si-Pc.

Figure 2. A) Summary of the absorption spectrum, B) Si-Pc, and C) HOMO-LUMO energy of Si-Pc with TD-DFT methods.

TD-DFT computation in the induced situation was used to observe the optical absorption behavior of Si-Pc. Molecular absorption structure and phenomenon are important factors for developing a device with photonic properties together with enhanced photostability. UV absorption bands affect the photostability of the device and are an important parameter.[31] In Fig. 2, the electronic absorption spectra of Si-Pc are combined and presented. In the UV region, the higher wavelength UV stability task is seen in the absorption bands of the molecule. The actual intermolecular charge transfer takes place inside the molecule as a result of the intermolecular contact. In this case, the maximum absorption behavior of Si-Pc is accurately captured. The maximum wavelength of the absorption band is known to grow with the HOMO-LUMO (π-π*) transition. The oscillatory strength of the current molecule is stronger (in the maximal absorption region). The increasing delocalization of π-electrons in the molecule is the cause of the absorption.[24] The wavelength shifts in Fig. 1,

which goes from yellow to red. Si-Pc's electronic absorption spectrum exhibits flexible electronic transitions between the transmitter and receiver and is stable with respect to the HOMO-LUMO energy (Figure 2).

A wide range of synthetic dyes have been developed for various applications, including in functional materials. In applications such as organic solar cells and near-infrared imaging, absorbers operating in the near-infrared (near-IR) region are in high demand.[32,33] In Figure 2A, the electronic absorption spectrum of the metal complex Pc is presented. Pcs with symmetrical π electron aromatic macrocycles are one of the best-known and most successful artificial dyes (Figure 2B). These applications utilise the unique optical properties of Pc, especially in the Q band, which can be arranged to meet expectations when known external substitutions are used.

In the Pc's chemistry, the Q band continues to be explored as one of the most interesting and fundamental topics.[34,35] Literature indicates that tailoring the absorption properties of Pc derivatives in the near-IR region involves broadening the π-conjugation by expanding the macrocyclic ring, which reduces the causes the Q band to divide.[36,37] In addition, the synthesis sequences resulting in discrete oligomers are generally long and yields are very low. To date, no Pc derivatives with a sharp Q band beyond 1000 nm have been reported, and the development of new strategies in this area is anticipated.[38] Here, the main group (Group 14) element was chosen as a substituent. This element has important aspects such as effective electronegativity and desirable orbital interactions. So this means that the inclusion of silicon atoms in Pc greatly affected the spectrum (Figure 2C). Here, the α-positions of group 14 (Si)-substituted Pc are presented in detail. A Pc with a certain symmetry was produced. In addition, it is aimed to avoid the influence of regional isomers and to understand the electronic properties as clearly as possible.

HOMO-LUMO levels and the distribution of electron density is a critical factor[39] affecting the reactivity of the molecule.[40,41] The quantum chemical properties of Si-Pc were determined by the DFT methods. E_{HOMO}, E_{LUMO}, E(Δ), and related parameters were calculated. The energy gap between the HOMO and LUMO levels (E_{HOMO}= -5.438 eV, E_{LUMO}= -3.630 eV, ΔE= 1.807 eV), ultimately resulting in redshifted spectra. Pc molecules in the Si-based monomer structure are expected to extend electronic conjugation due to orbital interaction between them. A reduction in molecular symmetry relevant values are listed in Table 1. Figure 3 provides graphic representations of HOMO, HOMO[1+], LUMO, and LUMO[1−]. The HOMO and LUMO energies were largely contributed by the C atoms in the molecule. Most of the atoms of Si-Pc contributed to the HOMO[1+] energy of the molecule. The LUMO[1−] the energy of the molecule came from nearly identical atoms, except for a few atoms in the region. HOMO energies: -5.460 eV, -5.031 eV, and -5.416 eV, and LUMO energies: -3.494 eV, -3.314 eV, and -3.228 eV respectively. The energy gap (Δ) transmits small excitation energies of the molecule. E(Δ) values are 1.965 eV, 1.717 eV, and 2.187 eV, respectively. In addition, thanks to the $λ_{max}$ value obtained in the experimental UV-visible spectroscopic analysis, the optical band gap[42] (Bandgap E(Δ) = $hc/λ_{max}$)of Si-Pc (http://physics.nist.gov/constants) was found to be 2.03 eV when calculated for 610 nm.[23] That is, the experimental and theoretically calculated optical band gaps are close to each other and less than 2.190 eV. The energy shift is sufficient to induce charge separation in the molecule reported here.
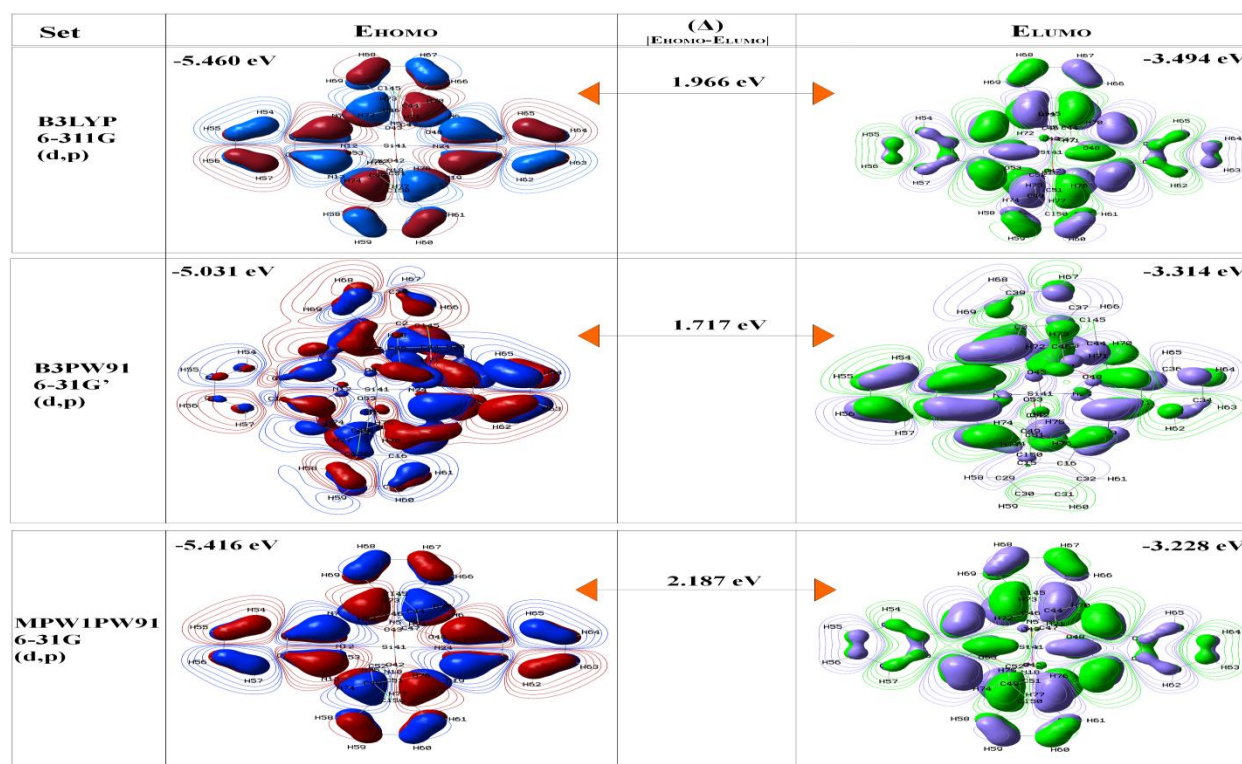

Figure 3. Atomic orbital comparison of Si-Pc.

According to Table 1, the ionization potential (I) of the molecules was calculated to be 5.460 using the B3LYP method, which represents the highest value among the methods analyzed. This indicates that the molecule obtained using this method has a lower tendency to lose electrons and exhibits greater stability compared to those obtained through other methods. The electron affinity (A), on the other hand, reached its highest value of 3.630 in the TD-DFT method, suggesting that the molecule has a stronger tendency to attract electrons relative to the results from the other methods. In terms of chemical hardness (η), the MPW1PW91 method produced the highest value of 1.094, signifying reduced chemical reactivity of the molecule. Conversely, the B3PW91 method demonstrated the highest chemical softness (s) value of 0.582, which implies that the molecule is more chemically reactive under this method. Regarding chemical potential (μ), the lowest value, -4.534, was obtained with the B3LYP method, highlighting the greater stability of the molecule under these conditions. When examining electronegativity (χ), the B3LYP method yielded the highest value of 2.315, reflecting a greater capacity of the molecule to attract electrons compared to those calculated through other methods. Finally, the electrophilicity index (ω) achieved its peak value of 11.37 with the B3LYP method, indicating a higher reactivity toward nucleophiles and a stronger electrophilic character than observed with the other methods. These findings suggest that the B3LYP method generally enhances the stability, electrophilic character, and electron-attracting capacity of the molecule. Furthermore, the interplay between chemical hardness and softness appears to play a critical role in determining the molecule's overall reactivity.

3.2. Dipole Moment Calculation of Si-Pc

The change in the dipole moment of organic semiconductors from soil to an excited state (Δμ) plays a significant role in the photovoltaic performance of solar cells.[43,44] As a typical charge-bearing material, axially substituted silicon (IV) phthalocyanine bearing the donor-acceptor type bis(3-chloropropanoate) will undergo local excitation when irradiated by sunlight to form a stable dipole state. Here, the dipole moment is measured in different methods (DFT and TD-DFT) were measured and compared. Si-Pc absorbs light; the resulting electronic transitions often lead to a red shift in absorption. These calculations provided information about the distribution of the electron cloud and molecular symmetry in the molecule. Here in Pcs, the donor-acceptor relationship is concentrated in the negative charge receiver unit part, and positive charge (electron-rich) in the donor unit part.

Molecular parameters for gas phase[45] Si-Pc; μ (D) = 7.97, 4.12, 7.75, and 8.03, α (au) = 512.12, 499.94, 891.78, and 513.94, β(esu) = 3.2 x 10^{-34}, 6.7 x 10^{-34}, 3.4 x 10^{-34}, and 3.1 x 10^{-34} was found respectively. For the chemical under investigation, these results suggest that they can be regarded as NLO materials (Table 2). Since different calculations of the molecule yielded the static high-order polarity β (esu) and polarity α (au) properties. The resulting data for Si-Pc seems to focus on photonic properties. Theoretically, high polarity values are taken stock to be a good candidate for nonlinear optical (NLO) materials. With this review, it is estimated that it can be used in applications in the field of solar cells.

Table 1. Energy gaps and energy properties for Si-Pc

Molecules Energy	DFT			TD-DFT
	B3LYP 6-311G (d,p)	B3PW91 6-31G' (d,p)	MPW1PW91 6-31G (d,p)	B3LYP 6-311G (d,p)
E_{LUMO}	-3.494	-3.314	-3.228	-3.630
E_{HOMO}	-5.460	-5.031	-5.416	-5.438
E_{LUMO+1}	-3.349	-3.188	-3.096	-3.230
E_{HOMO-1}	-7.053	-6.322	-7.095	-7.033
Energy Gap(Δ)	1.966	1.717	2.187	1.807
Ionization Potential(I)	5.460	5.031	5.416	5.438
Electron Affinity(A)	3.494	3.314	3.228	3.630
Chemical hardness(η)	0.983	0.858	1.094	0.904
Chemical softness(s)	0.508	0.582	0.457	0.553
Chemical Potential(μ)	-4.477	-4.172	-4.322	-4.534
Electronegativity(χ)	2.247	2.157	2.114	2.315
Electrophilicity index(ω)	10.05	10.14	8.53	11.37

Table 2. Parameters (debye, au, and esu) for gas phase Si-Pc.

Parameters	DFT			TD-DFT
	B3LYP 6-311G (d,p	B3PW91 6-31G' (d,p)	MPW1PW91 6-31G (d,p)	B3LYP 6-311G (d,p)
μ_x	-0.0002	-0.2580	0.0006	-0.0007
μ_y	0.0014	2.9834	-0.0029	0.0008

Int. J. Chem. Technol. **2025,** 9(1), 25-35.

Tanrıverdi and Yıldıko

μ_z	-7.9796	2.8414	-7.7595	-8.0366
μ (D)	7.9796	4.1281	7.7595	8.0366
α_{xx}	-292.51	-286.08	-281.96	-293.68
α_{yy}	-271.98	-271.22	-263.64	-271.39
α_{zz}	-354.81	-344.94	-346.89	-354.38
α_{xy}	-4.1129	1.4846	-4.3978	-4.4382
α_{xz}	-0.0007	-0.7665	0.0034	-0.0013
α_{yz}	0.0061	17.919	-0.0300	0.0042
α (au)	512.12	499.94	891.78	513.94
β_{xxx}	-0.0092	13.534	0.0525	0.0020
β_{xxy}	0.0225	29.005	-0.0817	0.0146
β_{xyy}	0.0074	-20.963	-0.0237	0.0061
β_{yyy}	0.0200	56.408	-0.0160	0.0091
β_{xxz}	-216.46	-22.996	-206.96	-223.30
β_{xyz}	-22.906	3.0083	-31.879	-27.016
β_{yyz}	-5.3884	78.814	-3.7719	5.9707
β_{xzz}	-0.0092	9.2771	0.0089	-0.0260
β_{yzz}	0.0159	26.673	-0.0436	0.0083
β_{zzz}	-88.034	40.611	-78.1705	-95.518
β (esu)	3.2×10^{-34}	6.7×10^{-34}	3.4×10^{-34}	3.1×10^{-34}

3.3. MEP Surface Features

Both the polarity and the reactivity of the molecule can be investigated by molecular electrostatic potential surface (MEPS) measurements.[46] The electrostatic potential on a molecule's surface is described by several colors. Looking at the map, the electron-rich region corresponds to the green area, which represents the neutral potential regions, the blue area, which describes the positive electrostatic potential regions, and the red area, which describes the negative electrostatic potential regions.[47] In DFT system MEPS maps of these compounds from different dimensional directions using is shown in Figure 4. As seen in the figure, the negative field concentrated around the oxygen atom is suitable as a donor. The positive domain represents the benzene and axially substituted silicon (IV) phthalocyanine groups. In this case, the molecule also exhibits an electron-accepting property. The molecule appears to have the best charge separation from the core to the edges. This indicates that charges can move efficiently in this molecule. So, as MEPS maps support the HOMO-LUMO findings, Si-Pc could be a suggestion for efficient solar cells application areas.

3.4. ELF for Si-Pc

Using the electron localization function (ELF) approximation, one can obtain a measure of the probability of locating an electron in proximity to another suitable electron. ELF is a useful method for mapping the probability of electron pair existence.[48] These maps show a direct separation in the shells between the nucleus and the valence electrons.[49] Si-Pc with dissociation energies is compatible with the Yamamoto model. It also helps to visualize

covalent bonds and lone pairs. This area is one of the higher growth areas recently. The two-dimensional projection of the ELF map shown in Figure 5 for the Si metal complex presents that the electron pairs are arranged close to the valence regions of both metal and carbon atoms. Only π molecular orbitals are considered to calculate ELF. Here, the confinement η in the regions between the Si and N atoms is rephrase to or greater than zero. One of the unexpected findings is that both chlorides are likely to favor shifts in the Si semi-metal, which would be caused by oxygen atoms.

ELF maps illustrate the localization of electron pairs, where values close to 1 indicate strong localization, whereas values near 0 suggest delocalization. The dark regions on the ELF map correspond to areas with high electron density. In the Si–N regions, ELF values approaching zero suggest low electron density, implying that these bonds may exhibit partial ionic character. Conversely, high ELF values observed in Si–metal and Si–carbon interactions highlight the covalent nature of these bonds. Additionally, the influence of chlorine atoms is supported by potential charge shifts, which are evident in the ELF map.

ELF analysis was employed to visualize the electron density distribution and bonding characteristics of the Si-Pc metal complex. The low ELF values in the region between Si and N atoms indicate that these bonds may possess a partially ionic character. In contrast, the high ELF values observed between Si and carbon atoms reinforce the covalent nature of these interactions. Furthermore, the ELF map reveals that chlorine atoms may induce a charge shift on the Si center. Overall, ELF analysis provides a clear depiction of the spatial distribution of electron pairs around the Si core and its surrounding atoms, contributing to a deeper understanding of the electronic structure of the metal complex.
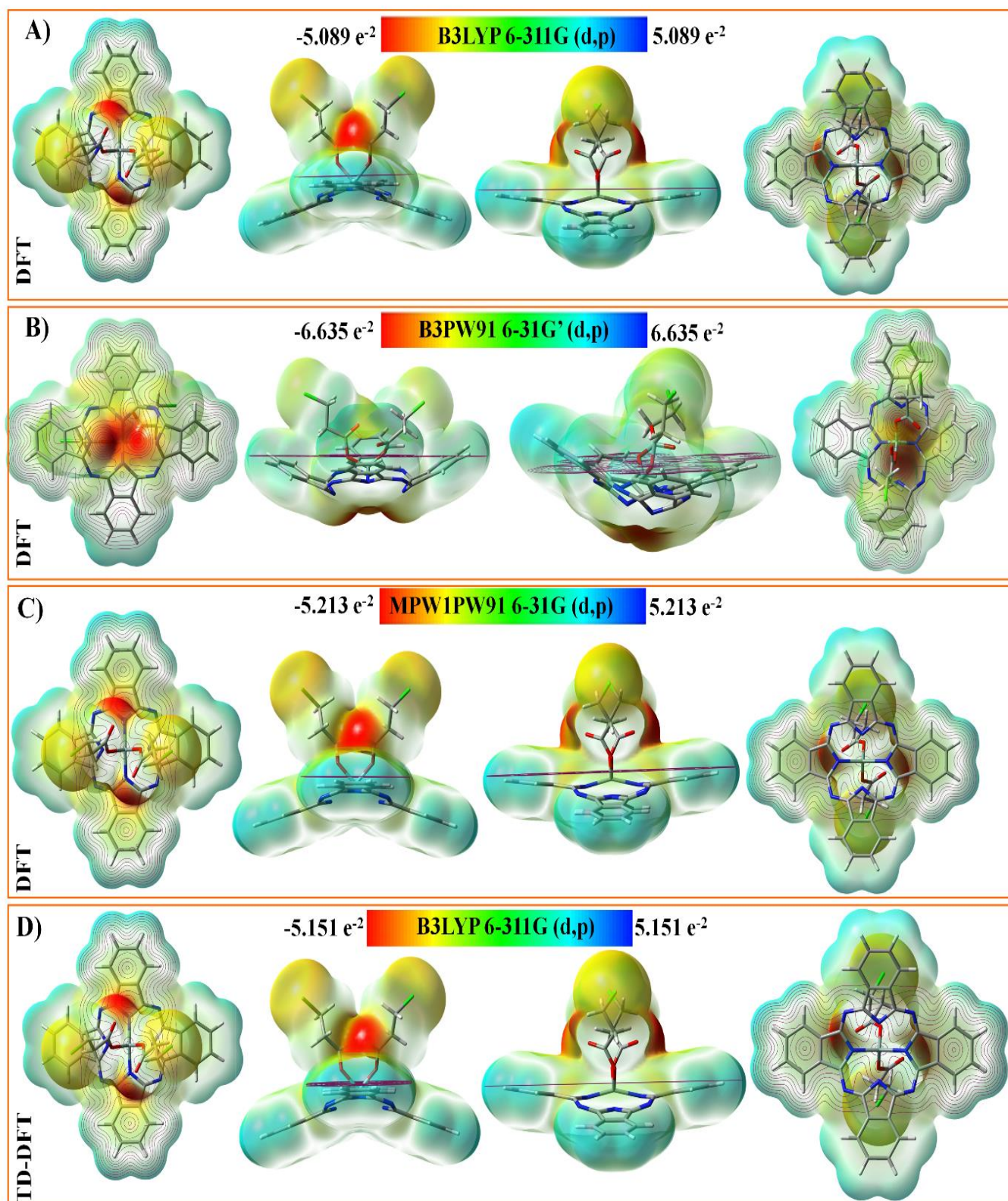
Figure 4. MEP maps of Si-Pc, obtained from different directions and different systems.
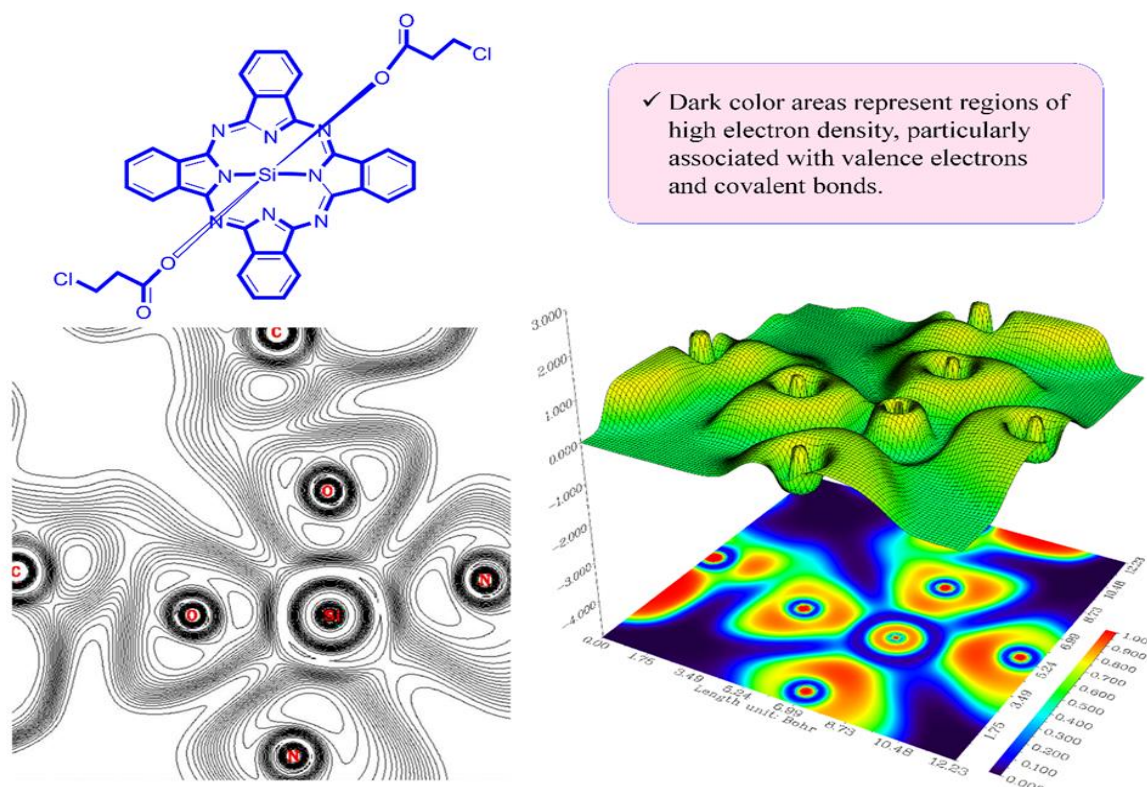
Int. J. Chem. Technol. **2025,** 9(1), 25-35.

Tanrıverdi and Yıldıko

✓ Dark color areas represent regions of high electron density, particularly associated with valence electrons and covalent bonds.

Figure 5. Electron localization function (ELF) analysis of Si-Pc was calculated on the B3LYP/6-311G (d,p) basis set of the DFT system.

4. CONCLUSION

In this study, energy and surface theoretical analyzes of the molecule were performed by DFT and TD-DFT methods. The electronic absorption spectra of the molecule were combined and presented. The extent to which the inclusion of the silicon atom in the Pc affects the spectrum is explained by the Q-Band. The α-positions of Group 14 (Si)-substituted Pc are presented in detail. In this study, a Pc with a certain symmetry is produced. As a result, experimental and theoretical values support each other. The combination of functionals and basis sets described in the simulations of all theoretical studies section was highly appropriate for the investigation of photonic properties. The employment of multiple functionals allowed for a more thorough assessment of different aspects of the system and facilitated the presentation of the computed values in a novel and distinctive manner within the context of existing literature. In particular, the use of B3LYP in conjunction with TD-DFT represents a well-established and widely preferred approach, known for producing reliable and consistent results. Theoretically, high polarity values were obtained. The compound can be considered to be a good candidate for NLO materials.

MEPS maps confirmed the HOMO-LUMO findings. With the ELF map, information was presented about the demarcation in the regions between Si and N atoms. The compound showed conductivity suitable for computational chemistry.

Conflict of interests

The authors declare no conflict of interest.

REFERENCES

1.Shibu, A.; Jones, S.; Tolley, P.L.; Diaz, D.; Kwiatkowski, C.O.; Jones, D.S.; Shivas, J.M.; Foley, J. J.; Schmedake, T.A. *Mater. Adv.* **2023**, 4 (23), 6321-6332.

2.Sweatha, L.; Aswathppa, S.; Chinnathambi, M.; Silviya, M.; Anithalakshmi, M.; Robert, R. *J. Mol. Struct.* **2024**, 1317, 139138.

3.Kim, S.; Quy, H. V.; Bark, C. W. *Mater. Today Energy* **2021**, 19, 100583.

4.Sachdeva, S.; Singh, D.; Tripathi, S. K. *Phys. Rev. B Condens.* **2024**, 695, 416552.

5.Wang, H.; Fukuda, T.; Ishikawa, N.; Matsuo, Y. *Org. Electron.* **2014**, 15 (1), 139-143.

6.Rozhkova, X.; Aimukhanov, A.; Zeinidenov, A.; Paygin, V.; Valiev, D.; Bisquert, J.; Guerrero, A.; Alexeev, A.; Ilyassov, B. *Synth. Met.* **2023**, 295, 117347.

7.Kabir, S.; Takayashiki, Y.; Ohno, A.; Hanna, J.-i.; Iino, H. *Opt. Mater.* **2022**, 126, 112209.

8.Küçükgenç, Ö.; Ağcaabat, R.; Dumludağ, F.; Odabaş, Z. *Polyhedron* **2024**, 262, 117169.

9.Balamurugan, G.; Park, J. S. *Dyes Pigments* **2022**, 201, 110199.

10.Lu, C.; Yu, Z.; Cao, J. *CJSC* **2024**, 43 (3), 100240.

11.Le, T.-H.; Tran, N.-A.; Fujii, A.; Ozaki, M.; Dao, Q.-D. *Thin Solid Films* **2023**, 787, 140134.

12.Gümrükçü Köse, G.; Karaoğlan, G. K.; Erdağ Maden, Y.; Koca, A. *Dyes Pigments* **2022**, 207, 110686.

13.Yüzer, A. C.; Kurtay, G.; Ince, T.; Yurtdaş, S.; Harputlu, E.; Ocakoglu, K.; Güllü, M.; Tozlu, C.; Ince, M. *Mater. Sci. Semicond. Process.* **2021**, 129, 105777.

14.Lawson Daku, L. M.; Casida, M. E. In *Green Chemistry and Computational Chemistry*, Mammino, L., Ed. Elsevier: 2022; pp 355-384.

15.Binnie, S. J.; Sola, E.; Alfè, D.; Gillan, M. J. *Mol. Simul.* **2009**, 35 (7), 609-612.

16.Viveros, A.; Rubio, E.; Mendoza, S.; Rodríguez, J.; Quintos, A. *SUSCOM* **2018**, 19.

17.Bello, S.; Urwick, A.; Bastianini, F.; Nedoma, A. J.; Dunbar, A. *Energy Rep.* **2022**, 8, 89-106.

18.Lamsabhi, A. M.; Yáñez, M.; Mó, O.; Trujillo, C.; Blanco, F.; Alkorta, I.; Elguero, J.; Caballero, E.;

30.Solgun, D. G.; Tanriverdi, A. A.; Yildiko, U.; Ağirtaş, M. S. *J. Incl. Phenom. Macrocycl. Chem.* **2022**, 102 (11), 851-860.

31.Wang, Y.; Li, T.; Ma, P.; Bai, H.; Chen, M.; Xie, Y.; Dong, W. *ACS Sustain. Chem. Eng.* **2016**, 4.

32.Choi, H.; Nicolaescu, R.; Paek, S.; Ko, J.; Kamat, P. V. *ACS Nano* **2011**, 5 (11), 9238-9245.

33.Kobayashi, N.; Furuyama, T.; Satoh, K. *J. Am. Chem. Soc.* **2011**, 133 (49), 19642-19645.

Rodriguez-Morgade, S.; Claessens, C.; Torres, T. *JPP* **2011**, 15, 1220-1230.

19.Nemykin, V.; Hadt, R.; Belosludov, V.; Mizuseki, H.; Kawazoe, Y. *J. Phys. Chem. A* **2007**, 111, 12901-13.

20.Jiang, X.; Gao, Y.; Lal, R.; Hu, J.; Song, B. *Mol. Phys.* **2018**, 116 (13), 1697-1705.

21.Savin, A.; Nesper, R.; Wengert, S.; Fässler, T. F. *Angew. Chem. Int. Ed.* **1997**, 36 (17), 1808-1832.

22.Fuentealba, P.; Chamorro, E.; Santos, J. C. *In Theoretical and Computational Chemistry*, Toro-Labbé, A., Ed. Elsevier: 2007; Vol. 19, pp 57-85.

23.Ağırtaş, M. S.; Ödemiş, Ö.; Solğun, D. G.; Tanrıverdı, A. A.; Özkartal, A. *J. Coord. Chem.* **2023**, 76 (11-12), 1471-1484.

24.Frisch, M.; Trucks, G.; Schlegel, H.; Scuseria, G.; Robb, M.; Cheeseman, J.; Scalmani, G.; Barone, V.; Mennucci, B.; Petersson, G., Gaussian Inc. *Wallingford Ct* **2009**, *2*.

25. 25.Frisch, M. J.; Trucks, G. W.; Schlegel, H. B.; Scuseria, G. E.; Robb, M. A……. et al. *Gaussian 16 Rev. C.01*, Wallingford, CT, 2016.

26.Tanriverdi, A. A.; Yildiko, U.; Tekes, A. T.; Cakmak, İ.; Ata, A. C. *Polym. Bull.* **2022**, 80, 9853–9880.

27.Sundaram, S.; Vijayakumar, V. N.; Balasubramanian, V. *Comput. Theor. Chem.* **2022**, 1217, 113920.

28.Alghamdi, S. K.; Abbas, F.; Hussein, R. K.; Alhamzani, A. G.; El-Shamy, N. T. *J. Mol. Struct.* **2023**, 1271, 134001.

29.Buvaneswari, M.; Santhakumari, R.; Usha, C.; Jayasree, R.; Sagadevan, S. *J. Mol. Struct.* **2021**, 1243, 130856.

34.de la Torre, G.; Vázquez, P.; Agulló-López, F.; Torres, T. *Chem. Rev.* **2004**, 104 (9), 3723-3750.

35.Namuangruk, S.; Sirithip, K.; Rattanatwan, R.; Keawin, T.; Kungwan, N.; Sudyodsuk, T.; Promarak, V.; Surakhot, Y.; Jungsuttiwong, S. *Dalton Trans.* **2014**, 43 (24), 9166-9176.

36.Hooper, R. W.; Zhang, A.; Koszelewski, D.; Lewtak, J. P.; Koszarna, B.; Levy, C. J.; Gryko, D. T.; Stillman, M. J. *JPP* **2018**, 22 (12), 1111-1128.

37. Karimova, N. V.; Luo, M.; Grassian, V. H.; Gerber, R. B. *PCCP* **2020**, 22 (9), 5046-5056.

38. Furuyama, T.; Satoh, K.; Kushiya, T.; Kobayashi, N. *J. Am. Chem. Soc.* **2014**, 136 (2), 765-776.

39. Yildiko, U.; Tanriverdi, A. A. *BKCS* **2022**, 43 (6), 822-835.

40. Valencia, D.; Whiting, G.; Bulo, R.; Weckhuysen, B. *PCCP* **2015**, 18.

41. Amudha, G.; Santhakumari, R.; Chandrika, D.; Mugeshini, S.; Rajeswari, N.; Sagadevan, S. *Chin. J. Phys.* **2022**, 76, 44-58.

42. Sefer, E.; Koyuncu, F. B. *Electrochim. Acta* **2014**, 143, 106-113.

43. Privado, M.; de la Cruz, P.; Malhotra, P.; Sharma, G. D.; Langa, F. *Sol. Energy* **2021**, *221*, 393-401.

44. Altun, K.; Yildiko, Ü.; Tanriverdi, A. A.; Çakmak, İ. *IJCT* **2021**, 5 (2), 147-155.

45. Włodarska, M.; Mossety-Leszczak, B. *Int. J. Mol. Sci.* **2021**, 22 (7), 3424.

46. Yildiko, U.; Tanriverdi, A. A. *J. Polym. Res.* **2021**, 29 (1), 19.

47. Scheiner, S., *J. Comput. Chem.* **2018**, 39 (9), 500-510.

48. Mierzwa, G.; Gordon, A. J.; Latajka, Z.; Berski, S. *Comput. Theor. Chem.* **2015**, 1053, 130-141.

49. Kansız, S.; Azam, M.; Dege, N.; Ermiş, N.; Al-Resayes, S. I.; Alam, M. *GCLR* **2022,** 15 (3), 825-836.